Estimating long-term groundwater storage and its controlling factors in Alberta, Canada

Soumendra N. Bhanja[1], Xiaokun Zhang[2], Junye Wang[1]

[1]Athabasca River Basin Research Institute (ARBRI), Athabasca University, 1 University Drive, Athabasca, Alberta T9S 3A3, Canada
[2]School of Computing & Information System, Athabasca University, 1 University Drive, Athabasca, Alberta T9S 3A3, Canada

Correspondence to: Junye Wang (junyew@athabascau.ca)

Abstract. Groundwater is one of the crucial natural resources for economic development and environmental sustainability particularly in Alberta, Canada. In this study, we estimated groundwater storage in 11 major river basins across Alberta, Canada using a combination of remote sensing (Gravity Recovery and Climate Experiment-GRACE), in situ surface water data, and land surface modelling estimates ($GWSA_{sat}$). We applied separate calculations for unconfined and confined aquifers, for the first time, to represent their hydrogeological differences. Storage coefficients for the individual wells were incorporated to compute the monthly in situ groundwater storage ($GWSA_{obs}$). The $GWSA_{sat}$ from the two satellite-based products were compared with $GWSA_{obs}$ estimates. The estimates of $GWSA_{sat}$ were in good agreement with the $GWSA_{obs}$ in terms of pattern and magnitude (e.g., RMSE ranged from 2 to 14 cm). While comparing $GWSA_{sat}$ with $GWSA_{obs}$, most of the statistical analyses provide mixed responses, however the Hodrick-Presscott trend analysis clearly showed a better performance of the GRACE-mascon estimate. The results showed trends of $GWSA_{obs}$ depletion in 5 of the 11 basins. Our results indicate that the precipitation played an important role in influencing the $GWSA_{obs}$ variation in 4 of the 11 basins studied. A combination of rainfall and snowmelt positively influence the $GWSA_{obs}$ in 6 basins. Water budget analysis showed an availability of comparatively lower terrestrial water in 9 of the 11 basins in the study period. Historical groundwater recharge estimates indicate a reduction of groundwater recharge in 8 basins during 1960-2009. The output of this study could be used to develop sustainable water withdrawal strategies in Alberta, Canada.

1 Introduction

Fresh water is an important resource for economic development and social sustainability around the world. Approximately, 1.2 billion people live in water scarce areas across the globe (UN-Water/FAO, 2007). More than a billion people lack access to safe drinking water and this number is increasing due to an increasing population (Connor, 2015). However, the effects of climate change on glaciers and snowpack, and human activities, such as over-use and over-extraction of resources, can result in lowering water tables and groundwater depletion (Scanlon et al., 2016; Bhanja et al., 2017b). In situ monitoring of wells is the traditional approach for estimating groundwater storage. However, well monitoring is spatially not continuous and has a

high cost at a large region. There are only scant observation stations in some areas, especially in semi-arid and arid environments, or cold climate regions covered by glacier and snowpack, due to difficulties of access and monitoring. As a result, proper groundwater management and decision-making are hampered considerably by the scarcity of data.

Remote sensing data from the Gravity Recovery and Climate Experiment (GRACE) satellite mission could be used to estimate groundwater storage at a continuous and large scale across the globe, and offers a new opportunity for groundwater storage assessment (Rodell et al., 2007). Although the GRACE satellite mission currently provides global-scale data for the detection of temporal gravity changes (Tapley et al., 2004), these temporal gravity changes are not a direct measurement of groundwater storage. A relationship would have to be established between temporal gravity changes and groundwater storage variations through the continuously evolving algorithms (Watkins et al., 2015). Estimates of groundwater storage using the remote sensing have been performed around the globe (Swenson et al., 2006; Rodell et al., 2007; Strassberg et al., 2007; Rodell et al., 2009; Tiwari et al., 2009; Scanlon et al., 2012; Shamsudduha et al., 2012; Voss et al., 2013; Bhanja et al., 2014; Richey et al., 2015; Panda and Wahr, 2016; Bhanja et al., 2016; Chen et al., 2016; Long et al., 2016; Bhanja et al., 2017b; Bhanja et al., 2018). Huang et al. (2016) used remote sensing data for computing the groundwater storage anomalies (GWSA) in order to estimate groundwater storage in Alberta. They used ground water levels at 36 wells, mostly confined to the southern Alberta region, and were correlated with both the GRACE total water storage (TWS) and groundwater storage (GWS) variations. Then they compared the TWS with groundwater levels instead of the groundwater storage and without considering surface water data due to the lack of available high resolution data.

Recent studies (e.g. Huang et al., 2015; Nanteza et al., 2017) have considered both confined and unconfined aquifers for in situ GWSA computation but they have not separated the data from the two types. The two types of aquifers have different recharge and storage patterns. Confined aquifers are overlain by relatively impermeable rock or clay, which limits vertical water infiltration, while in unconfined aquifers, vertical water infiltration can occur from precipitation, snowmelt, surface water etc. The two types of aquifers are also responding differently with effect from pumping (Alley et al., 1999). Therefore, these should be studied separately for estimating groundwater storage at a region. Further, Rodell et al. (2007) indicated the importance of surface water factors in the GWSA estimation and sought for inclusion of surface water storage variations in GWSA disaggregation. They also pointed out the importance of separating contributions to temporal mass variability using auxiliary observations and numerical models when estimating groundwater storage changes in large scale regions. In cold climate regions, such as in Alberta, the surface water could make a significant contribution to groundwater storage variations due to the effects of climate change on snowpack, glaciers, permafrost, and wetlands. Therefore, more efforts are required to properly evaluate groundwater storage for aquifer storage coefficients in transforming groundwater level information to groundwater storage in cold climate regions (Feng et al., 2013). The main objectives of this study are:

1. To investigate the long term groundwater storage conditions in cold climate regions, such as the 11 river basins in Alberta, Canada, by combining all of the processing steps, such as the surface water storage estimates.

2. To validate the remote sensing estimates from two different remote sensing products using the maximum available in situ observation well data. The in situ groundwater storage has been estimated by combining the storage coefficients and aquifer thickness (for confined aquifers) with the water table fluctuation.
3. To find the role of natural hydrological components (e.g. precipitation, snowmelt, evapotranspiration) for influencing groundwater storage variations. We have also studied long-term groundwater recharge trends from a global-scale hydrological model for inferring long-term variabilities in groundwater recharge rates.

2 Materials and Methods

2.1 Study area

This study has been conducted in the major river basins (the map has been made following Lemay and Guha, 2009; AEP, 2011; AEP, 2017) within the province of Alberta (Figure 1a, 1b). The Peace River basin is the largest basin in the province, followed by the Athabasca River basin and Hay River basin, respectively (Table 1). Most parts of the study region have been characterized as the cold climate region (Peel et al., 2007). Basin-scale, annual average precipitation varies within 330 to 570 mm/year (Table 1). We used Global Land Cover Facility (GLCF) native resolution data (resolution: ~460 m × 460 m; www.landcover.org) for characterizing land cover (Channan et al., 2014). Most of the land areas in Alberta are covered by natural vegetation (i.e. Forest, Shrubland, mixture of Shrub and Grassland (MSG), and Grassland; Figure 1c, Table S1). The second most prevalent land-cover type is cropland (Figure 1c, Table S1). Surface water bodies (water and permanent wetland) cover less than 6% of the area of all the river basins (Figure 1c, Table S1).

We used monthly mean precipitation data from the archives of the Climatic Research Unit (CRU), University of East Anglia. The quality controlled, gridded $0.25^0 \times 0.25^0$, monthly mean TS4.0 total precipitation products are used here (Harris et al., 2014). The precipitation-gauge based data was collected through the World Meteorological Organization (WMO), National Oceanographic and Atmospheric Administration (NOAA), as well as other international and national agencies across the globe for preparing this dataset (Harris et al., 2014). The precipitation data are spatially averaged in order to provide basin-scale data. CRU data have been found to have the best match of other available products while comparing with in situ precipitation measurements in China (Zhao and Fu, 2006). Precipitation data exhibits temporal as well as spatial variations in the study period with values of 150 mm/year to >1000 mm/year (Figure 2). In general, the lowest precipitation has been observed in 2004 and the highest in 2010 (Figure 2). Spatially averaged basin-scale precipitation values indicate the highest precipitation rates prevail in the North Saskatchewan River basin (basin 4, 573 mm/year; Table 1) and lowest rates prevail in the South Saskatchewan River basin (basin 9, 334 mm/year; Table 1). Precipitation rates are highly seasonal in Alberta (Figure 3).

2.2 In situ measurements of groundwater storage

Groundwater level (GWL) depth data are obtained from the Alberta Environment and Parks, Government of Alberta (http://environment.alberta.ca/apps/GOWN/#). Daily GWL depth data are obtained for 470 monitoring wells distributed across the province of Alberta. Out of 470 available groundwater level monitoring locations, data recording intervals in approximately two third of the wells are intermittent during the study period. Therefore, we applied a filter of at least 80% of the temporal data availability at any locations for their further usage in our analyses within the study period 2003-2015, resulting in the use of GWL data from 157 measurement locations. Daily GWL information is converted to monthly GWL at individual locations. Because of the differences in GWS variations within different types of aquifers, these wells need to be classified as unconfined, semi-confined and confined. Out of the 157 measurement locations used in the study, 24 are located in unconfined aquifers, 17 are located within semi-confined aquifers, 100 are located within confined aquifers and 16 are unclassified (Figure 1d). Basin-wide details of distribution of wells are provided in Table S2. The screen depth of the wells varies from 6 m to 220 m (Figure 1e). The wells located in unclassified or semi-confined aquifers are characterized as either confined or unconfined based on their location hydrogeology and screen depth. For example, a well screened at a semi-confined aquifer with shallower depth and underlain by permeable materials, can be classified as an unconfined aquifer for storage calculations and vice versa.

We have studied the subsurface hydrogeology in detail using well-specific lithology information from the Alberta Environment and Parks, Government of Alberta (http://environment.alberta.ca/apps/GOWN/#). In order to compute groundwater storage anomalies ($GWSA_{obs}$) in an unconfined aquifer, the GWSA needs to be accurately represented using the storage coefficients of the aquifer (Scanlon et al., 2012). We have followed the equation (Todd and Mays, 2005; Bhanja et al., 2017a):

$$GWSA_{obs} = (h_m \times S_y - h_i \times S_y) \quad (1)$$

Where, h_m and h_i represent the mean GWL depth and GWL depths at different time periods at a location; S_y represents the specific yield of the aquifer. S_y is assigned to the individual data based on the specific yield of the geologic material in its screen position. Specific yield data corresponding to a specific geologic material are presented in Table S3.

$GWSA_{obs}$ in a confined aquifer have been estimated following the equation (Todd and Mays, 2005):

$$GWSA_{obs} = (h_m \times S_s \times b - h_i \times S_s \times b) \quad (2)$$

Where, S_s is the specific storage and b is the thickness of the aquifer. S_s of a material varies over a wide range, the details of material-specific S_s are provided in Table S4. Thickness of the aquifer for the individual aquifer units is obtained from the Alberta Environment and Parks, Government of Alberta. The data are assigned to individual wells based on their screening zone and thickness of the particular aquifer unit.

2.3 Surface water storage processing

Surface water level daily time-series are obtained (n= 393) from the Water Office, Government of Canada (wateroffice.ec.gc.ca) for the study region. After rearranging the data based on near-continuous data availability, we used 65 locations with > 80% of the data availability range. The data are temporally averaged at each location for estimating monthly mean values. The number of locations that fall within each of the river basins are spatially averaged to obtain the month-scale spatially averaged surface water anomaly. The surface water coverage fraction varies over the study region (Figure 1c and Table S1). In order to get realistic surface water storage variations, surface water area fractions have been multiplied with the spatially averaged surface water anomaly in each river basin.

2.4 Gravity recovery and climate experiment (GRACE)

We have obtained the monthly mean liquid water equivalent thickness, $1^0 \times 1^0$ gridded data from the archives of the National Aeronautics and Space Administration's (NASA) Jet Propulsion Laboratory (JPL). JPL-mascon solutions, version RL05, was used for 137 months (the data were not available for some of the months, details can be found in Watkins et al., 2015) between January 2003 and April 2015. The GRACE mission observes changes in gravity in the Earth's subsurface and provide the data on a continuous basis. The gravity change information has been processed further in order to obtain the terrestrial water storage (TWS) change data (details can be found here: http://grace.jpl.nasa.gov/data/get-data/jpl_global_mascons/ accessed on 14 November, 2017). Satellite Laser Ranging (SLR) has been incorporated for estimating degree 2 and order 0 coefficients (Cheng and Tapley, 2004). Processes to improve the geocenter correction have been reported by Swenson et al. (2008). The Glacial isostatic adjustment (GIA) related post glacial rebound signals are removed using the process by Geruo et al. (2013). In the mascon approach, the entire globe is characterized as equally-spaced 3^0 spherical mass concentration blocks (Watkins et al., 2015). In order to improve the TWS estimates, scale factors provided with the data are multiplied (Bhanja et al., 2016). Scale factors are estimated in order to improve the performance of the TWS estimates.

The spherical harmonics (SH) related TWS information has been obtained for 137 months (between January 2003 and April 2015) from the NASA JPL archive. We used $1^0 \times 1^0$ gridded RL05 data sets of SH solutions (Landerer and Swenson, 2012). Three independent solutions from the Center for Space Research at the University of Texas at Austin, the NASA JPL, and the German Space Agency (GFZ), were retrieved and combined to use in this study. Like the mascon approach, several similar techniques are applied to obtain the TWS change in the SH approach (Source: http://grace.jpl.nasa.gov/data/get-data/monthly-mass-grids-land/ accessed on 14 November, 2017). Errors associated with N-S stripes in the TWS data are removed using a destriping filter. A Gaussian filter at 300-km width is also applied to the data. In order to improve the TWS estimates, the scale factor provided with the data are multiplied (Bhanja et al., 2016).

One advantage of the mascon approach is the introduction of *a priori* information that leads to the removal of correlated noise (stripes) in the data. As a result, post-processing filters are not required to be applied (Watkins et al., 2015). TWS data

obtained from the mascon approach are less dependent on scale factors for estimating basin-scale mass change estimates (Watkins et al., 2015).

2.5 Estimating groundwater storage from remote sensing and global models

Satellite-based groundwater storage anomalies ($GWSA_{sat}$) are estimated using a mass balance approach after removing other components of the hydrological cycle from the TWSA. These components include soil moisture anomaly (SMA), anomalies in snow water equivalents (SNA), and anomalies in surface water variations (SWA). Anomalies are estimated after removing the all-time mean value from the individual monthly values for all of the components. Soil moisture and snow water equivalents data were retrieved from NASA's Global Land Data Assimilation System (GLDAS) (Rodell et al., 2004) for 148 months in the study period. The GLDAS include observation data from satellite sensors and ground-based measurements in order to improve the simulation output (Rodell et al., 2015). Bhanja et al. (2016) reported better GWSA estimates while using a combination of data from simulations of three different land surface models (LSM), comparing the use of any single model's output. We also used a combined estimate from the outputs of the Community Land Model (CLM), Variable Infiltration Capacity (VIC), and Noah (Rodell et al., 2004). Surface water variation plays an important role in estimating GWSA. We have computed the surface water variations using in situ data, described in section 2.3. GWSA can be estimated using the following equation:

$$GWSA_{sat} = TWSA - SMA - SNA - SWA \quad (3)$$

2.6 Groundwater recharge from global-scale hydrological model

In order to find the historical groundwater recharge pattern, we used a global-scale hydrological model, WaterGAP (version 2.2) (Döll et al., 2014) to estimate long-term groundwater recharge data (1960-2009). The WaterGAP simulates global-scale water storage and transport including human water use and groundwater recharge from surface water bodies at $0.5^0 \times 0.5^0$ resolution (Döll et al., 2014). Water withdrawal from both groundwater and surface water have also been considered. We used a combination of diffuse groundwater recharge and recharge from the surface water bodies, which we termed as "total groundwater recharge". As the WaterGAP simulation consider simple water balance approach for groundwater recharge estimation, uncertainties may arise as a function of groundwater table gradient (Döll et al., 2014). Furthermore, increasing groundwater recharge from surface water bodies as a function of groundwater withdrawal, has not been considered here (Döll et al., 2014). More information on model processes, data used and other details can be found in Döll et al. (2014).

2.7 Statistical approaches

In order to compare the datasets using statistically robust techniques, we have used the root mean square error (RMSE), Pearson's correlation, skewness, kurtosis, and the coefficient of variation. RMSE has been used to show the departures from the true (in situ estimates here) value (Helsel and Hirsch, 2002). The trend analyses are based on the linear regression analysis. In order to represent the non-linearity present within the data, we used the Hodrick-Prescott (HP) filter (Hodrick

and Prescott, 1997), a non-parametric, non-linear trend analysis. The HP filter employs a specific approach for separating trend (T_t) and cycle (c_t) components in the data (y_t).

$$y_t = T_t + c_t \quad (4)$$

In order to estimate the trend and cycle separately, the HP filter solves the following equation (Hodrick and Prescott, 1997):

$$\text{Min (T)} \sum_{t=1}^{T}((y_t - T_t)^2 + \lambda((T_{t+1} - T_t) - (T_t - T_{t-1}))^2 \quad (5)$$

Where T_{t+1} and T_{t-1} represents the trend component with time steps of *t+1* and *t-1*, respectively. The long term average of the cyclical components is close to zero (Hodrick and Prescott, 1997). The smoothing parameter (λ) is a positive number that reduces the variability within cyclical components (Hodrick and Prescott, 1997). The value of λ was chosen to be 14400 for monthly data (Hodrick and Prescott, 1997; Ravn and Uhlig, 2002).

2.8 Assumptions and limitations

On the basis of data availability, we have not included the entire extent of the river basins (Figure 1a) in the current analysis. The river basins are selected based only on their geopolitical extent in the province of Alberta (Figure 1b). For in situ estimates, GWSA information is spatially averaged for providing the basin's GWSA estimates and also to compare them with the satellite-based estimates following Bhanja et al. (2017a) and Scanlon et al. (2018) etc. The time-period of the study is restricted by the availability of data. Separation of GWSA signals from TWSA by removing all other components is a challenging task due to the lack of in situ measurements of other components and the large uncertainties associated with LSM simulated products (Scanlon et al., 2015). We have shown the satellite-based estimates for all of the basins, however, users should be cautious to use GRACE data in the smallest basins. This is because GRACE's native resolution could not allow users to directly use the data for smaller basins. Other processes, such as, the use of GRACE and integrated land surface model's operation could make the data available to use for smaller basins (Landerer and Swenson, 2012; Watkins et al., 2015). Data processing methods Proposed by Dutt Vishwakarma et al. (2016) could be used to make the data available for smaller basins with GRACE-SH products.

3 Results and Discussions

3.1 Groundwater storage anomalies

In situ GWSA ($GWSA_{obs}$) values ranged from -30 to 30 cm in all of the basins, with the highest fluctuations observed in basin 7. $GWSA_{obs}$ exhibits near zero values in basins 5, 6, 10 and 11 (Figure 3). $GWSA_{obs}$ magnitudes in different basins can arise as a result of diversity in specific yield values in the underlying material (Table S3). In situ estimates show seasonality, i.e. variations with precipitation rates etc., in basin 7. Trends in the $GWSA_{obs}$ show decreasing GWSA between 2003 and 2015 in basins 2, 3, 7, 8 and 9 (Table 1). The results indicate that $GWSA_{obs}$ depletion is in the range of -0.20 in basins 2 and 3. It is interesting to note that the basins 7, 8 and 9 are composed of >25% cropland (Table S1). Basin 3 has been subjected

to the highest amount of licensed groundwater withdrawal allocation in Alberta (basin 3 accounts for 39% of the total groundwater usage in Alberta). On the other hand, an increasing trend has been observed in the remaining basins (Table 1). One probable cause for the groundwater table increase in these basins could be related to precipitation variability. The study region has been subjected to large-scale drought during 1999-2005 (Hanesiak et al., 2011). As a result, the TWS recovery in 2004-2007 has also been observed by Lambert et al. (2013).

Another important factor influencing groundwater recharge as well as the groundwater storage, is the snowmelt processes prevailing in cold regions during the onset of spring-summer. The river basins have been receiving substantial amount of snowfall during winter months (Figure 3). This leads to snow accumulation in the region. At the end of winter season, snowmelt processes are majorly accounting for our observation of increasing GWSA in April onwards (Figure 3). The observation is in line with the observations from the earlier studies conducted within the study region (Hayashi and Farrow, 2014; Hood and Hayashi, 2015). Comparatively higher rates of precipitation during summer months and the snowmelt during the start of the summer season, are the major processes responsible for the observation of higher GWSA during summertime at the entire study region (Figure 3).

$GWSA_{obs}$ values from the unconfined aquifers reflect higher magnitude than that in the confined aquifers (Figure S1). This is because of the intrinsic property of the different types of aquifers. For instance, dewatering from the saturated zone during a pumping event, is mainly responsible for the release of water in unconfined aquifer (Alley et al., 1999). On the other hand, a net decrease in groundwater potential and associated reduction in water pressure have been occurred during a pumping event in a confined aquifer. The indigenous water expands slightly due to the decrease in water pressure, leading to slight compression in the aquifer material (Alley et al., 1999). This can explain why the groundwater storage change in the confined aquifers are comparatively lower than that in the unconfined aquifers.

Remote sensing estimates of GWSA ($GWSA_{sat}$) using the two different assessments, GRACE-MS and GRACE-SH approaches, show temporal variations ranging from -20 to 20 cm. However, the seasonal amplitudes are not similar in different basins (Figure 3). In general, the magnitude of the $GWSA_{sat}$ compares well with that of the $GWSA_{obs}$ (Figure 3). $GWSA_{sat}$ exhibits large amplitudes in basins 4, 7 and 8 (Figure 3). In general, the $GWSA_{sat}$ estimates from the two products match well with the observed estimates (Figure 3). The estimations are in line with the values reported for the Mackenzie River basin by Scanlon et al. (2018). Overall, the two satellite based estimates are found to be closely matching with one another, detailed comparisons are provided in section 3.2.

3.2 Comparison between observed and satellite-based GWSA

Deviations from the observed values are measured by the root mean squared error (RMSE) that combines both bias and lack of precision (Helsel and Hirsch, 2002). The RMSE estimates show a good match of satellite-based GWSA estimates in comparing the in situ estimates. RMSE was found to be within 5 cm in most of the basins (Figure 4a). In general, both of the satellite-based estimates exhibit similar RMSE in basins 2, 3, 5, 6 and 11 (Figure 4a). Pearson's correlation coefficient (r) provides information on the linear association between the two variables (Helsel and Hirsch, 2002). Comparing the two

products, correlation coefficients are found to be higher for the MS product in most of the basins (Figure 4b). Skewness has been used to represent the symmetricity in the data distribution (Helsel and Hirsch, 2002) and kurtosis has been used to represent the tail length of data distribution. Skewness and kurtosis have been used here in order to compare the GWSA estimates from the two satellite-based estimates with the in situ estimate. Comparing the two estimates, skewness and kurtosis analyses provide mixed results. For example, one product provides better results in some of the basins, the other in the remaining basins (Figure 4c, 4d).

Data dispersion can be measured through the coefficients of variation (CV). In general, CV data are found to match well for the two satellite-based products and the in situ estimates (Figure 5). CV data shows mixed responses when comparing the two satellite-based estimates. Scatter analysis shows the characteristic of the relationship (i.e. linear, non-linear) between the two variables (Helsel and Hirsch, 2002). Scatter analysis results do not provide any distinct comparison between the MS, SH estimates and the in situ estimate (Figure 6). The in situ data contains signatures of individual wells and, as a result, are influenced by local-scale climatic, hydrogeologic, and anthropogenic responses. However, the satellite-based estimates are providing responses from a large region and may not be influenced by local-scale fluctuations (Bhanja et al., 2016).

We used a non-parametric filtering (HP filter) approach for computing the trends in GWSA and compared the results with in situ estimates. HP trends of $GWSA_{obs}$ show the recent depleting trends in basins 1, 2, 3, 7 and 9 (Figure 7). In general, the HP trends of satellite-based estimates are relatively similar to each other. However, a comparatively better match of GWSA for the GRACE-MS product and in situ estimates has been observed in basins 4, 5, 6, 10 and 11. Significantly negative (*p value* <0.01) correlation has been observed for both estimates in basins 7, 8 and 9, which are subjected to irrigation with >25% land area coverage affected (Figure 1b and Table S1).

3.3 Precipitation and snowmelt influence on GWSA

In general, precipitation is the major controlling factor for variations in water storage (Scanlon et al., 2012). In this study, we have observed that GWSA values are not directly influenced by the precipitation pattern in some of the basins (Figure 8). The HP trend analysis shows a good match of $GWSA_{obs}$ with precipitation in basins 1 and 10 only (Figure 8, Table S5). $GWSA_{obs}$ trends are not following precipitation pattern in other basins (Figure 8, Table S5). The cross-correlation analysis between HP trends provide similar inferences (Table S5). In order to investigate the relationship with more detail, the Granger causality analyses (Granger, 1988) were performed with order 1 (insignificant results were found when other orders were used). Results show precipitation significantly (*p value* <0.01) causes $GWSA_{obs}$ in 4 of the 11 studied basins, basin 1, 5, 7 and 11. The results were found to be insignificant or even negatively correlated in other basins (Table S5).

A part of the precipitation, in particular, snowfall has little influence in modulating the groundwater storage, unless it is converted to snowmelt water. Therefore, we have studied the combined influence of rainfall and snowmelt water on $GWSA_{obs}$ without considering the direct snowfall amount. The rainfall and the snowmelt water data are retrieved from the three LSMs (CLM, VIC and Noah) in GLDAS archive and used in combination. Good match between rainfall and snowmelt water, and $GWSA_{obs}$ have been obtained in basins 1 and 11. Cross-correlation analyses indicate similar inference (Table S6).

Granger causality analyses (order 1) show the combined effect of rainfall and snowmelt water significantly causes $GWSA_{obs}$ in 6 basins: 1, 2, 5, 7, 9 and 11 respectively.

3.4 GWSA and the natural water budget

Observation of a non-significant relationship of precipitation, snowmelt water and GWS anomalies in most of the basins indicated the influence of other factors controlling GWS. In this aspect, the natural water availability for terrestrial water components (i.e. groundwater, surface water, soil moisture, etc.) have been studied by delineating the difference (DIFF) between precipitation (P) and evapotranspiration (ET) in another way, called the net precipitation flux (Syed et al., 2005; Rodell et al., 2015). Long et al. (2014) found outputs from LSMs provide the best ET estimates comparing in situ observations. We retrieved data from the simulation of the Noah land surface model, version 2.1, as a part of the GLDAS simulation (Rodell et al., 2004). The DIFF data exhibit negative values during summer months (Figure 9). Comparatively lower P and higher ET values are observed in the summer months, making the DIFF negative. The basin-wise DIFF values show reducing estimates in 9 of the 11 basins with the highest being observed in the Peace River basin (basin 2), where the DIFF estimate shows a net reduction of 0.41 km^3 of water between 2003 and 2015 (Table 1). Reduction in DIFF values is putting stress on terrestrial water as well as groundwater conditions in the study region. We have studied the long-term (1960-2009) groundwater recharge occurrence from the global-scale model output because of unavailability of direct groundwater recharge measurement in the region. The simulated, historical total groundwater recharge was found to be negative in 8 out of 11 basins, suggesting a change in rechargeable water volume. Groundwater storage, being a combination of recharge from precipitation, snowmelt water and surface water bodies; the inter-aquifer flow, discharge to surface water bodies and the anthropogenic withdrawal, could be largely impacted from reductions of the first three terms. Increasing human activities linked with groundwater withdrawal could lead to severe groundwater stress if it continues uncontrolled.

4 Conclusions

A network of 157 daily groundwater monitoring wells was used to compute groundwater storage anomalies (GWSA) in 11 major river basins in Alberta, Canada between January 2003 and April 2015. Well-specific hydrogeology information and separate treatment of the unconfined and confined aquifers were used for the calculation. Results show that the GWSA trends exhibit depletion in some of the basins that are dominated by anthropogenic groundwater withdrawal, either from irrigational use or domestic and industrial uses. A GWSA depletion rate has been observed as high as -0.20 cm/year in the Athabasca River basin. The GWSA estimates obtained from remote-sensing probes provided opportunities to evaluate groundwater conditions in remote, ungauged regions. We used two recently released satellite products for estimating $GWSA_{sat}$ in the studied basins. A combination of surface water measurements (n=393) and land surface model estimates of soil moisture and snow water equivalents were used. In general, the remote sensing estimates are in good agreement with that of the observed estimates, implying that remote sensing estimates could be used in future to monitor groundwater

storage in the region at a near-continuous rate. We have investigated the influence of precipitation and snowmelt water on GWSA variations. Results show that precipitation caused significant GWSA variations in 4 out of 11 studied basins. A combination of rainfall and snowmelt water causes significant GWSA variations in 6 basins, indicating prevalence of other factors for influencing GWSA in the remaining basins. Water budget analysis of terrestrial water availability show reductions of available water during the study period in 9 basins. Results indicate groundwater recharge rates have been decreasing from 1960-2009 in 8 of the basins studied. Outputs of this study may be used to frame sustainable water withdrawal strategies in Alberta, keeping in mind the available water for groundwater recharge.

Acknowledgements and Data

The authors would like to thank the Alberta Economic Development and Trade for the Campus Alberta Innovates Program Research Chair (No. RCP-12-001-BCAIP). We would also like to thank Mr. Jim Sellers for the proofreading. This study uses open-source data from the Groundwater Observation Well Network (GOWN), Alberta Environment and Perks. Surface water data were obtained from the Water Office, Government of Canada (wateroffice.ec.gc.ca). Climatic Research Unit's (CRU) precipitation data were obtained from the CRU achieves from the University of East Anglia. GRACE land data were processed by Sean Swenson, supported by the NASA MEaSUREs Program, and is available at http://grace.jpl.nasa.gov. The GLDAS data used in this study were acquired as part of the mission of NASA's Earth Science Division and archived and distributed by the Goddard Earth Sciences (GES) Data and Information Services Center (DISC). The WaterGAP model outputs are retrieved from the University of Frankfurt archive: https://www.uni-frankfurt.de/45217892/datensaetze.

References

Alberta Environment and Perk (AEP): Groundwater use, pp 5 (http://aep.alberta.ca/about-us/documents/FocusOn-GroundwaterUse-2014.pdf accessed on November 21, 2017), 2011.

Alberta Environment and Perk (AEP): (http://aep.alberta.ca/water/programs-and-services/water-for-life/water-supply/water-allocation-management/water-quantity.aspx accessed on November 21, 2017), 2017.

Alley, W.M., Reilly, T.E. and Franke, O.L.: Sustainability of ground-water resources, US Department of the Interior, US Geological Survey, 1186, 1999.

Bhanja, S., Mukherjee, A., Rodell, M., Velicogna, I., Pangaluru, K., and Famiglietti, J. S.: Regional groundwater storage changes in the Indian Sub-Continent: the role of anthropogenic activities, In: American Geophysical Union, Fall Meeting, GC21B-0533, 2014.

Bhanja, S. N., Mukherjee, A., Saha, D., Velicogna, I. and Famiglietti, J. S.: Validation of GRACE based groundwater storage anomaly using in situ groundwater level measurements in India, Journal of Hydrology, 543, 729-738, 2016.

Bhanja, S. N., Rodell, M., Li, B., Saha, D., and Mukherjee, A.: Spatio-temporal variability of groundwater storage in India, Journal of Hydrology, 544, 428-437, 2017a.

Bhanja, S. N., Mukherjee, A., Rodell, M., Wada, Y., Chattopadhyay, S., Velicogna, I., Pangaluru, K., and Famiglietti, J. S.: Groundwater rejuvenation in parts of India influenced by water-policy change implementation, Scientific Reports, 7, 7453, 2017b.

Bhanja, S. N., Mukherjee, A. and Rodell, M.: Groundwater Storage Variations in India, In Groundwater of South Asia, Springer, Singapore, 49-59, 2018.

Channan, S., Collins, K. and Emanuel, W. R.: Global mosaics of the standard MODIS land cover type data, University of Maryland and the Pacific Northwest National Laboratory, College Park, Maryland, USA, 2014.

Chen, J. L., Wilson, C. R., Tapley, B. D., Scanlon, B., and Güntner, A.: Long-term groundwater storage change in Victoria, Australia from satellite gravity and in situ observations, Global and Planetary change, 139, 56-65, 2016.

Cheng, M., and Tapley, B. D.: Variations in the Earth's oblateness during the past 28 years, J. Geophys. Res., 109, B09402, doi:10.1029/2004JB003028, 2004.

Connor, R.: The United Nations world water development report 2015: water for a sustainable world (Vol. 1), UNESCO Publishing, 2015.

Döll, P., Mueller Schmied, H., Schuh, C., Portmann, F. T., and Eicker, A.: Global-scale assessment of groundwater depletion and related groundwater abstractions: Combining hydrological modeling with information from well observations and GRACE satellites, Water Resources Research, 50(7), 5698-5720, 2014.

Dutt Vishwakarma, B., Devaraju, B. and Sneeuw, N.: Minimizing the effects of filtering on catchment scale GRACE solutions, Water Resources Research, 52, 5868-5890, 2016.

Feng, W., Zhong, M., Lemoine, J.M., Biancale, R., Hsu, H.T. and Xia, J.: Evaluation of groundwater depletion in North China using the Gravity Recovery and Climate Experiment (GRACE) data and ground-based measurements, Water Resources Research, 49(4), 2110-2118, 2013.

Geruo, A., Wahr, J., and Zhong, S.; Computations of the viscoelastic response of a 3-D compressible Earth to surface loading: an application to Glacial Isostatic Adjustment in Antarctica and Canada, Geophys. J. Int. 192, 557–572, 2013.

Goldin, T.: Groundwater: India's drought below ground, Nature Geoscience, 9, 98-98, 2016.

Granger, C. W.: Some recent development in a concept of causality. Journal of econometrics, 39, 199–211, 1988.

Hanesiak, J. M., Stewart, R. E., Bonsal, B. R., Harder, P., Lawford, R., Aider, R., Amiro, B. D., Atallah, E., Barr, A. G., Black, T. A., and Bullock, P.: Characterization and summary of the 1999–2005 Canadian Prairie drought. Atmosphere-Ocean, 49, 421-452, 2011.

Harris, I. P. D. J., Jones, P. D., Osborn, T. J. and Lister, D. H.: Updated high-resolution grids of monthly climatic observations–the CRU TS3. 10 Dataset, International Journal of Climatology, 34, 623-642, 2014.

Hayashi, M. and Farrow, C. R.: Watershed-scale response of groundwater recharge to inter-annual and inter-decadal variability in precipitation (Alberta, Canada), Hydrogeology Journal, 22, 1825-1839, 2014.

Helsel, D. R., and Hirsch, R. M.: Statistical methods in water resources, Vol. 323. Elsevier, 2002.

Hodrick, R. J., and Prescott, E. C.: Postwar US business cycles: an empirical investigation, J. Money Credit Bank., 1–16, 1997.

Hood, J. L. and Hayashi, M.: Characterization of snowmelt flux and groundwater storage in an alpine headwater basin, Journal of Hydrology, 521, 482-497, 2015.

Huang, Z., Pan, Y., Gong, H., Yeh, P. J. F., Li, X., Zhou, D. and Zhao, W.: Subregional-scale groundwater depletion detected by GRACE for both shallow and deep aquifers in North China Plain, Geophysical Research Letters, 42, 1791-1799, 2015.

Huang, J., Pavlic, G., Rivera, A., Palombi, D. and Smerdon, B.: Mapping groundwater storage variations with GRACE: a case study in Alberta, Canada, Hydrogeology Journal, 24,1663-1680, 2016.

Lambert, A., Huang, J., Kamp, G., Henton, J., Mazzotti, S., James, T. S., Courtier, N. and Barr, A. G.: Measuring water accumulation rates using GRACE data in areas experiencing glacial isostatic adjustment: The Nelson River basin, Geophysical Research Letters, 40, 6118-6122, 2013.

Landerer, F. W., Swenson, S. C.: Accuracy of scaled GRACE terrestrial water storage estimates, Water Resour. Res., 48, W04531, 2012.

Long, D., Longuevergne, L. and Scanlon, B.R.: Uncertainty in evapotranspiration from land surface modeling, remote sensing, and GRACE satellites, Water Resources Research, 50(2), 1131-1151, 2014.

Long, D., Chen, X., Scanlon, B. R., Wada, Y., Hong, Y., Singh, V. P., Chen, Y., Wang, C., Han, and Z., Yang, W.: Have GRACE satellites overestimated groundwater depletion in the Northwest India Aquifer? Sci. Rep. 6, 2016.

Lemay, T. G. and Guha, S.: Compilation of Alberta groundwater information from existing maps and data sources ERCB/AGS Open File Report 2009-02, ISBN 978-0-7785-6969-5 (http://ags.aer.ca/document/OFR/OFR_2009_02.PDF accessed on November 21, 2017), 2009.

Nanteza, J., de Linage, C. R., Thomas, B. F. and Famiglietti, J. S.: Monitoring groundwater storage changes in complex basement aquifers: An evaluation of the GRACE satellites over East Africa, Water Resources Research, 52, 9542–9564, 2016.

Panda, D. K., and Wahr, J.: Spatiotemporal evolution of water storage changes in India from the updated GRACE-derived gravity records, Water Resour. Res., 51, doi:10.1002/2015WR017797, 2016.

Peel, M.C., Finlayson, B.L. and McMahon, T.A.: Updated world map of the Köppen-Geiger climate classification, Hydrology and earth system sciences, 11, 1633-1644, 2007.

Ravn, M. O., and Uhlig, H.: On adjusting the Hodrick-Prescott filter for the frequency of observations, Review of economics and statistics, 84, 371-376, 2002.

Richey, A. S., Thomas, B. F., Lo, M.- H., Famiglietti, J. S., Reager, J. T., Voss, K., Swenson, S., and Rodell, M.: Quantifying renewable groundwater stress with GRACE, Water Resour. Res. 51, 5217–5238, 2015.

Rodell, M. et al.: The global land data assimilation system. Bull. Am. Meteorol. Soc. 85 (3), 381–394. http://dx.doi.org/10.1175/BAMS-85-3-381, 2004.

Rodell, M., Chen, J., Kato, H., Famiglietti, J.S., Nigro, J., Wilson, C.: Estimating groundwater storage changes in the Mississippi River basin (USA) using GRACE, Hydrogeol. J., 15, 159–166, 2007.

Rodell, M., Velicogna, I., Famiglietti, J. S.: Satellite-based estimates of groundwater depletion in India, Nature, 460, 999–1002, 2009.

Rodell, M., et al.: The observed state of the water cycle in the early twenty-first century, J. Clim., 28, 8289–8318, doi:10.1175/JCLI-D-14-00555.1, 2015.

Scanlon, B. R., Longuevergne, L. and Long, D.: Ground referencing GRACE satellite estimates of groundwater storage changes in the California Central Valley, USA, Water Resour. Res., 48, W04520, doi:10.1029/2011WR011312, 2012.

Scanlon, B. R., Zhang, Z., Reedy, R. C., Pool, D. R., Save, H., Long, D., Chen, J., Wolock, D. M., Conway, B. D. and Winester, D.: Hydrologic implications of GRACE satellite data in the Colorado River Basin, Water Resources Research, 51, 9891-9903, 2015.

Scanlon, B. R., Zhang, Z., Save, H., Wiese, D. N., Landerer, F. W., Long, D., Longuevergne, L. and Chen, J.: Global evaluation of new GRACE mascon products for hydrologic applications, Water Resour. Res, 52, 9412-9429, 2016.

Scanlon, B. R., et al.: Global models underestimate large decadal declining and rising water storage trends relative to GRACE satellite data, Proceedings of the National Academy of Sciences, 201704665, 2018.

Shamsudduha, M., Taylor, R.G., Longuevergne, L.: Monitoring groundwater storage changes in the Bengal Basin: validation of GRACE measurements, Water Resour. Res. 48, W02508. http://dx.doi.org/10.1029/2011WR010993, 2012.

Strassberg, G., Scanlon, B. R., and Rodell, M.: Comparison of seasonal terrestrial water storage variations from GRACE with groundwater-level measurements from the High Plains Aquifer (USA), Geophys. Res. Lett. 34, L14402. http://dx.doi.org/10.1029/2007GL030139, 2007.

Syed, T.H., Famiglietti, J.S., Chen, J., Rodell, M., Seneviratne, S.I., Viterbo, P. and Wilson, C.R.: Total basin discharge for the Amazon and Mississippi River basins from GRACE and a land-atmosphere water balance, Geophysical Research Letters, 32(24) 2005.

Swenson, S. P., Yeh, J. -F., Wahr, J., Famiglietti, J.: A comparison of terrestrial water storage variations from GRACE with in situ measurements from Illinois, Geophys. Res. Lett. 33, L16401. http://dx.doi.org/10.1029/2006GL026962, 2006.

Swenson, S. C., Chambers, D. P., Wahr, J.: Estimating geocenter variations from a combination of GRACE and ocean model output, J. Geophys. Res.-Solid Earth 113, (B8). http://dx.doi.org/10.1029/2007JB005338 Article B08410, 2008.

Tapley, B. D., Bettadpur, S., Ries, J. C., Thompson, P. F., Watkins, M. M.: GRACE measurements of mass variability in the Earth system, Science, 305, 503–505, 2004.

Tiwari, V. M., Wahr, J., and Swenson, S.: Dwindling groundwater resources in northern India, from satellite gravity observations, Geophys. Res. Lett., 36, L18401, 2009.

Todd D. K. and Mays L. W.: Groundwater hydrology, 3rd edition, John Wiley & Sons, NJ, pp. 636, 2005.

Voss, K. A., Famiglietti, J. S., Lo, M., de Linage, C., Rodell, M., and Swenson, S. C.: Groundwater depletion in the Middle East from GRACE with implications for transboundary water management in the Tigris-Euphrates-Western Iran region, Water Resour. Res., 49, 2013.

Watkins, M. M., Wiese, D. N., Yuan, D. -N., Boening, C., and Landerer, F. W.: Improved methods for observing Earth's time variable mass distribution with GRACE using spherical cap mascons, J. Geophys. Res. Solid Earth 120. http://dx.doi.org/10.1002/2014JB011547, 2015.

UN-Water/FAO: World Water Day: Coping with Water Scarcity: Challenge of the twenty-first century. (http://www.fao.org/nr/water/docs/escarcity.pdfaccessed on November 21, 2017) , 2007.

Zhao, T. and Fu, C.: Comparison of products from ERA-40, NCEP-2, and CRU with station data for summer precipitation over China, Advances in Atmospheric sciences, 23, 593-604, 2006.

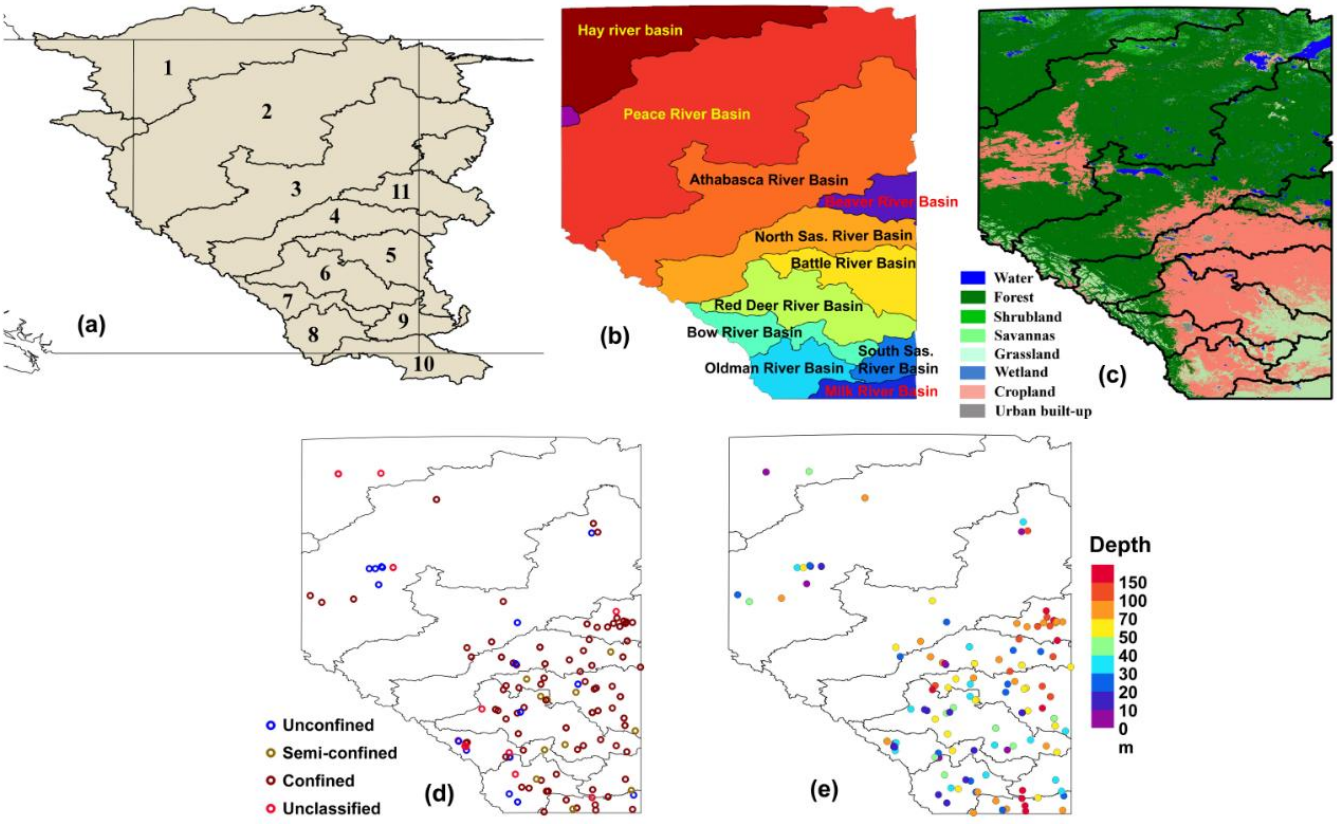

Figure 1: Major river basins in Alberta, (a) full basin extent; (b) Alberta only; (c) dominant land cover types; (d) aquifer types represented through the studied wells; (e) depth of wells screened in Alberta, overlaid by basin boundaries

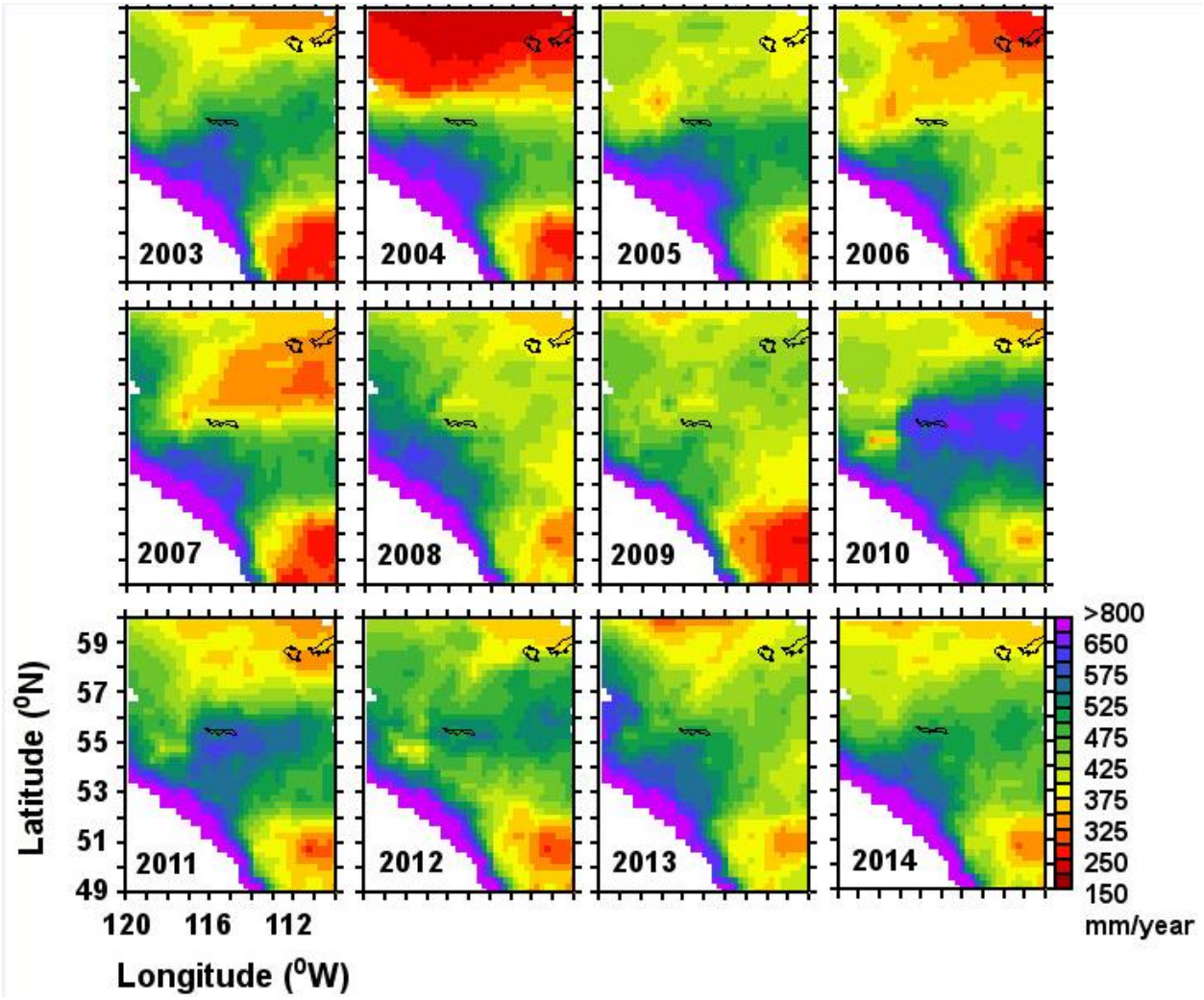

Figure 2: Annual precipitation rates (mm/year) in Alberta between 2003 and 2014

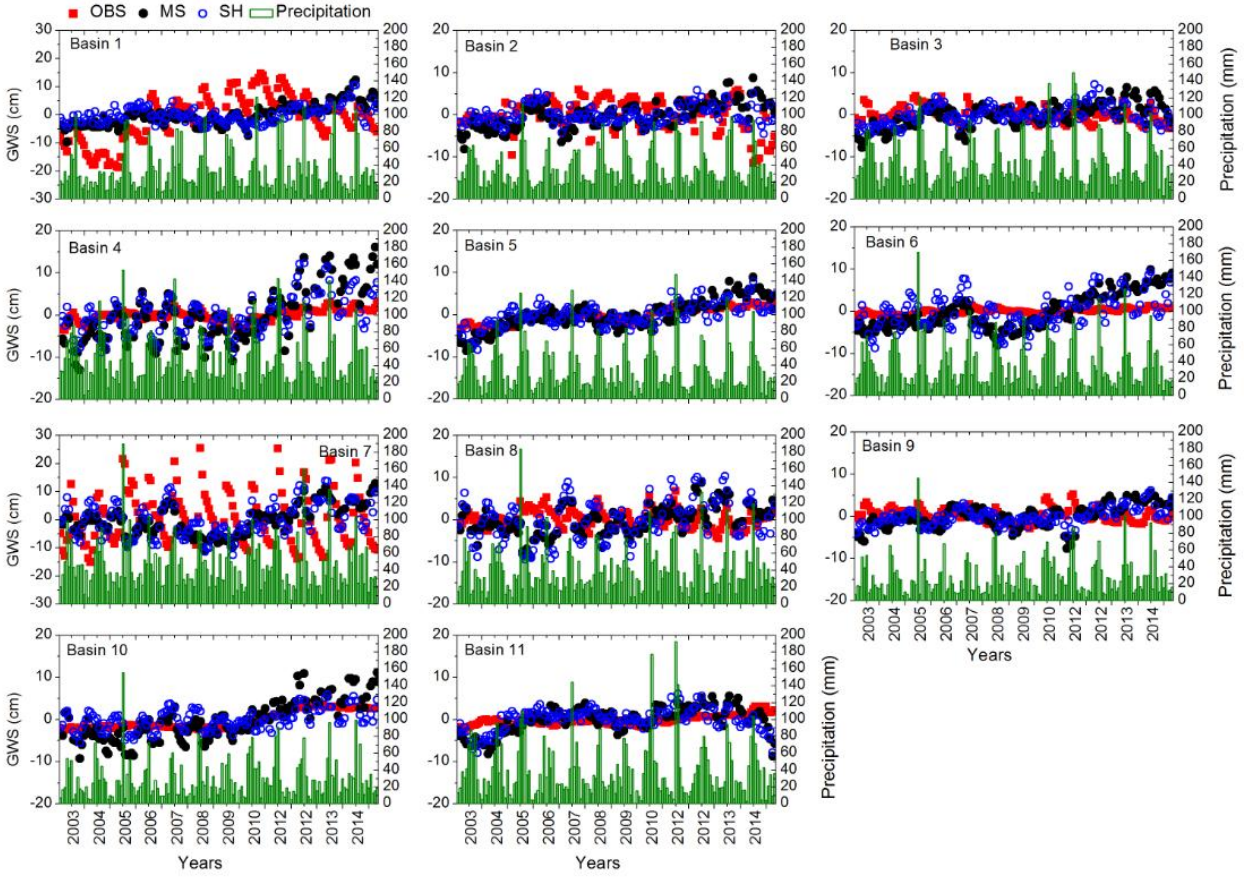

Figure 3: Basin-wide, monthly time-series of in situ GWSA (OBS, red squares), GWSA obtained using GRACE mascon product (MS, black filled circles) and GRACE SH products (SH, blue open circles), respectively. Monthly, spatial averaged precipitation data are shown using green columns

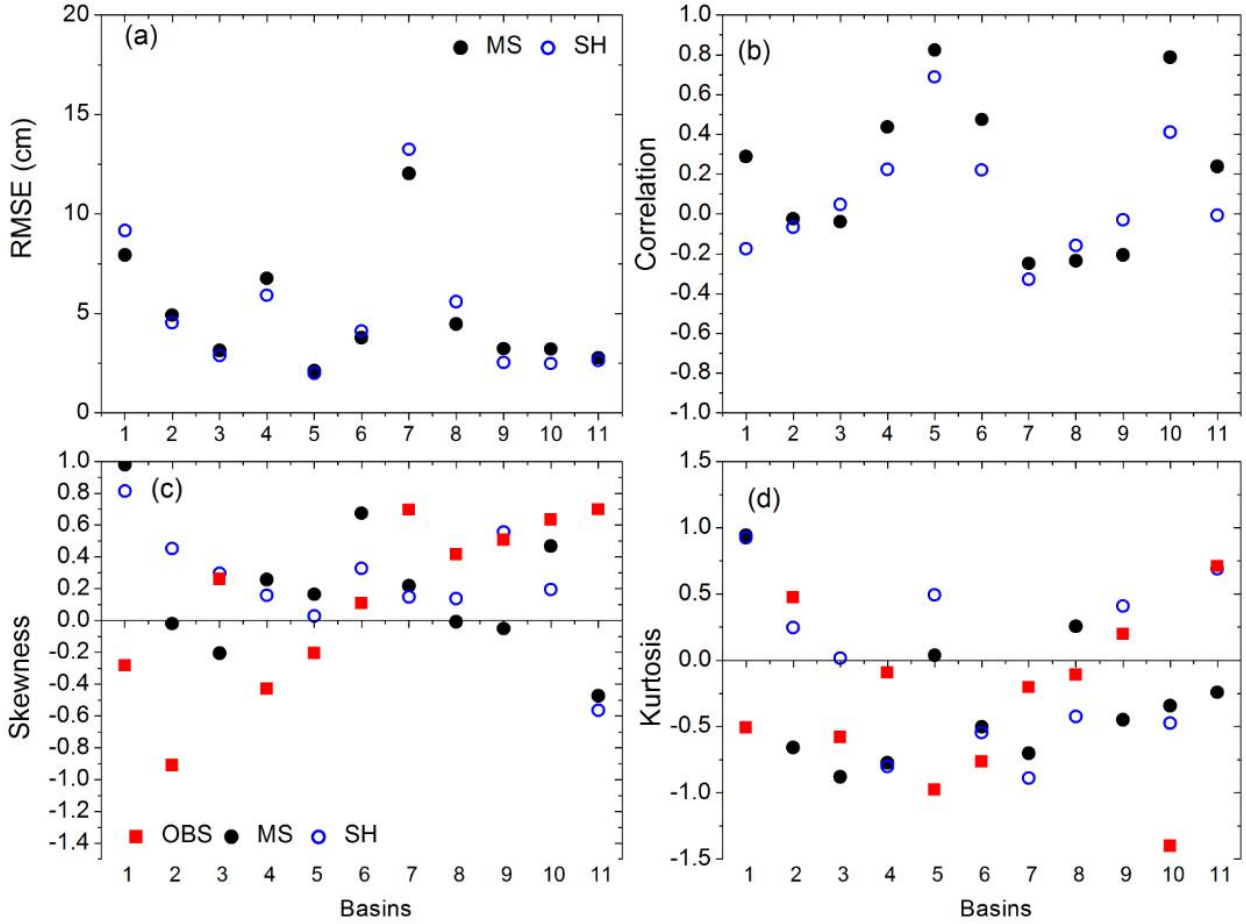

Figure 4: Basin-wide estimates of (a) RMSE; (b) correlation; (c) skewness and (d) kurtosis

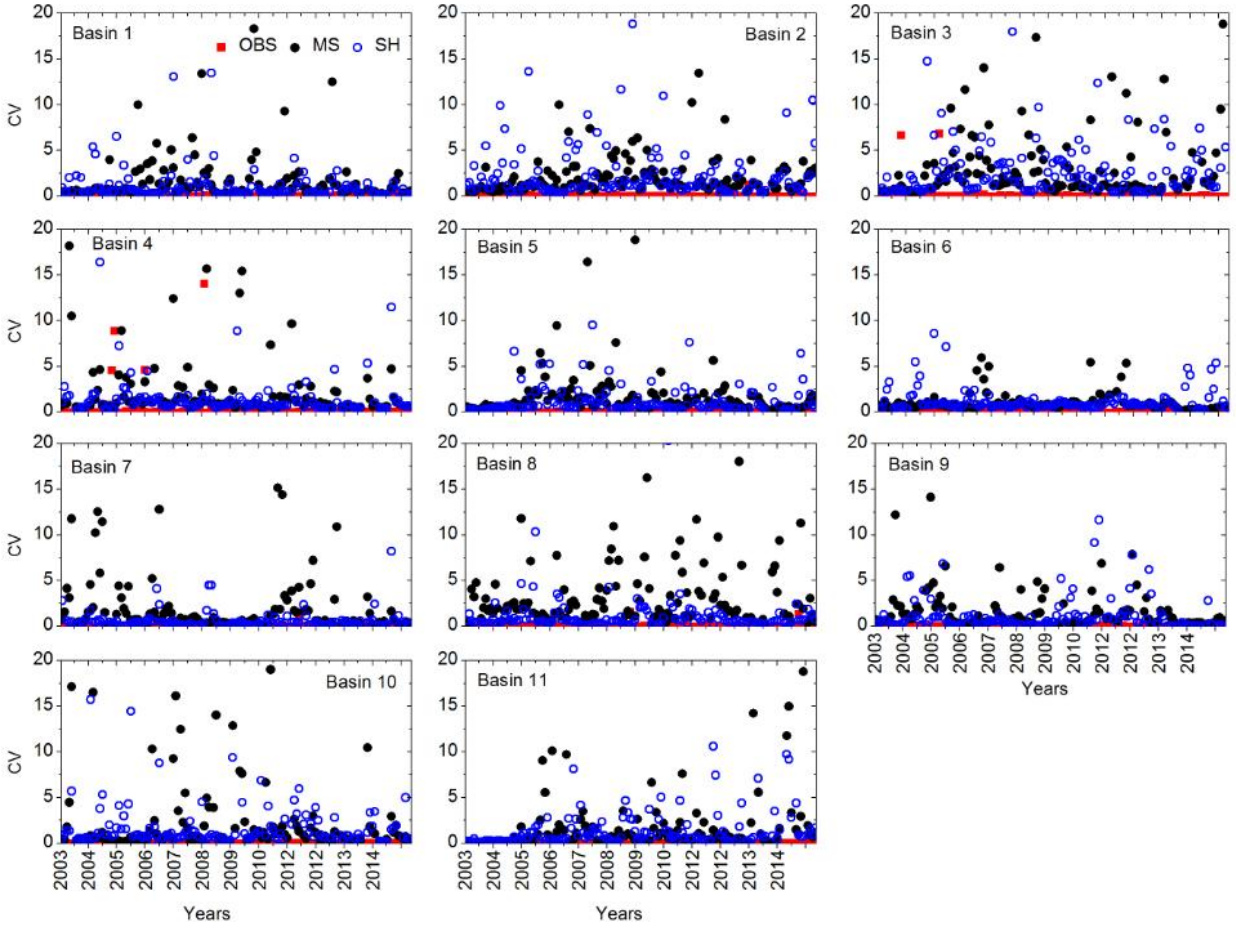

Figure 5: Basin-wide coefficient of variation (CV) analysis for in situ GWSA (OBS, red squares), GWSA obtained using GRACE mascon product (MS, black filled circles) and GRACE SH products (SH, blue open circles), respectively

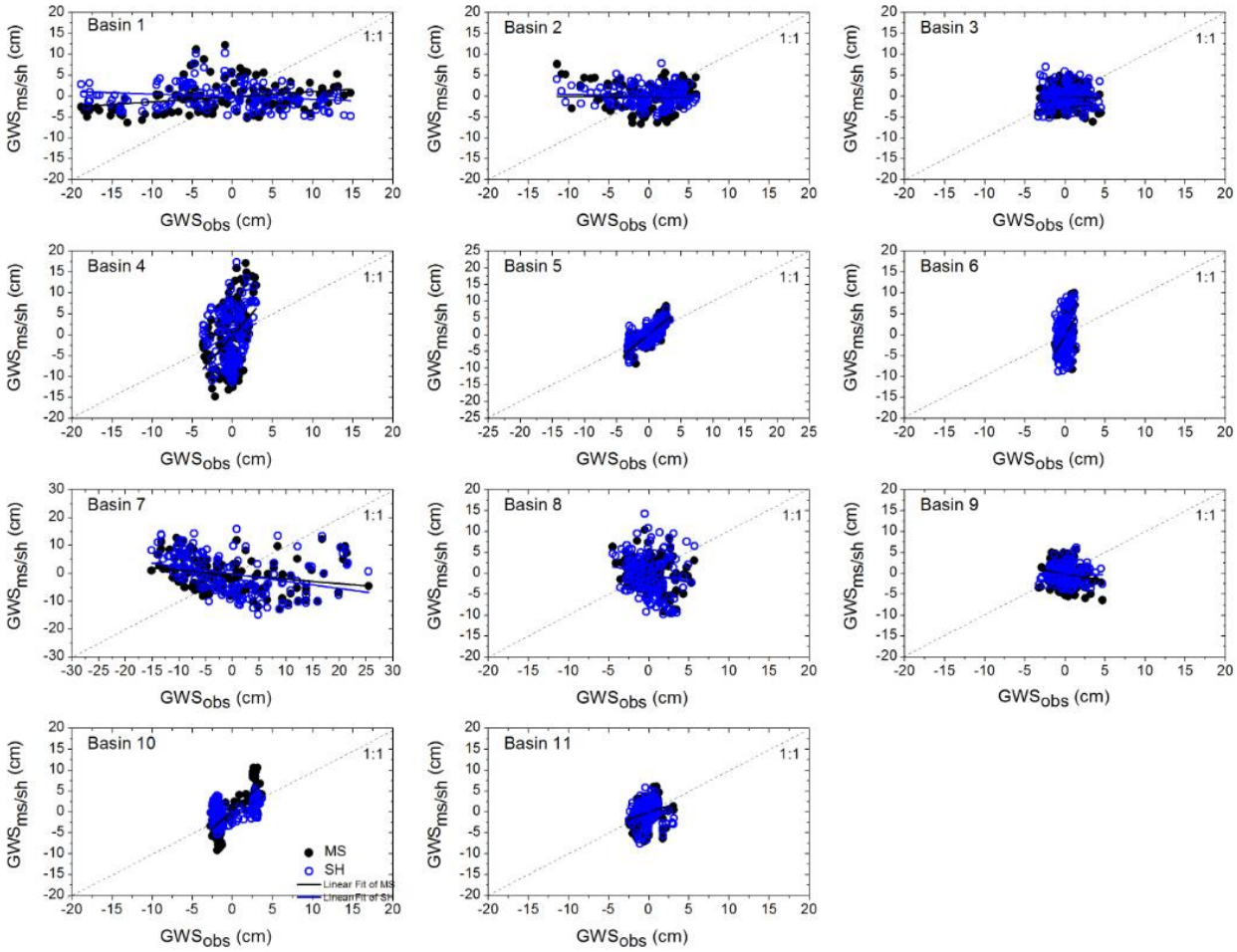

Figure 6: Basin-wide scatter analysis of in situ GWSA with the GWSA obtained using GRACE mascon product (MS, black filled circles) and GRACE SH products (SH, blue open circles), respectively

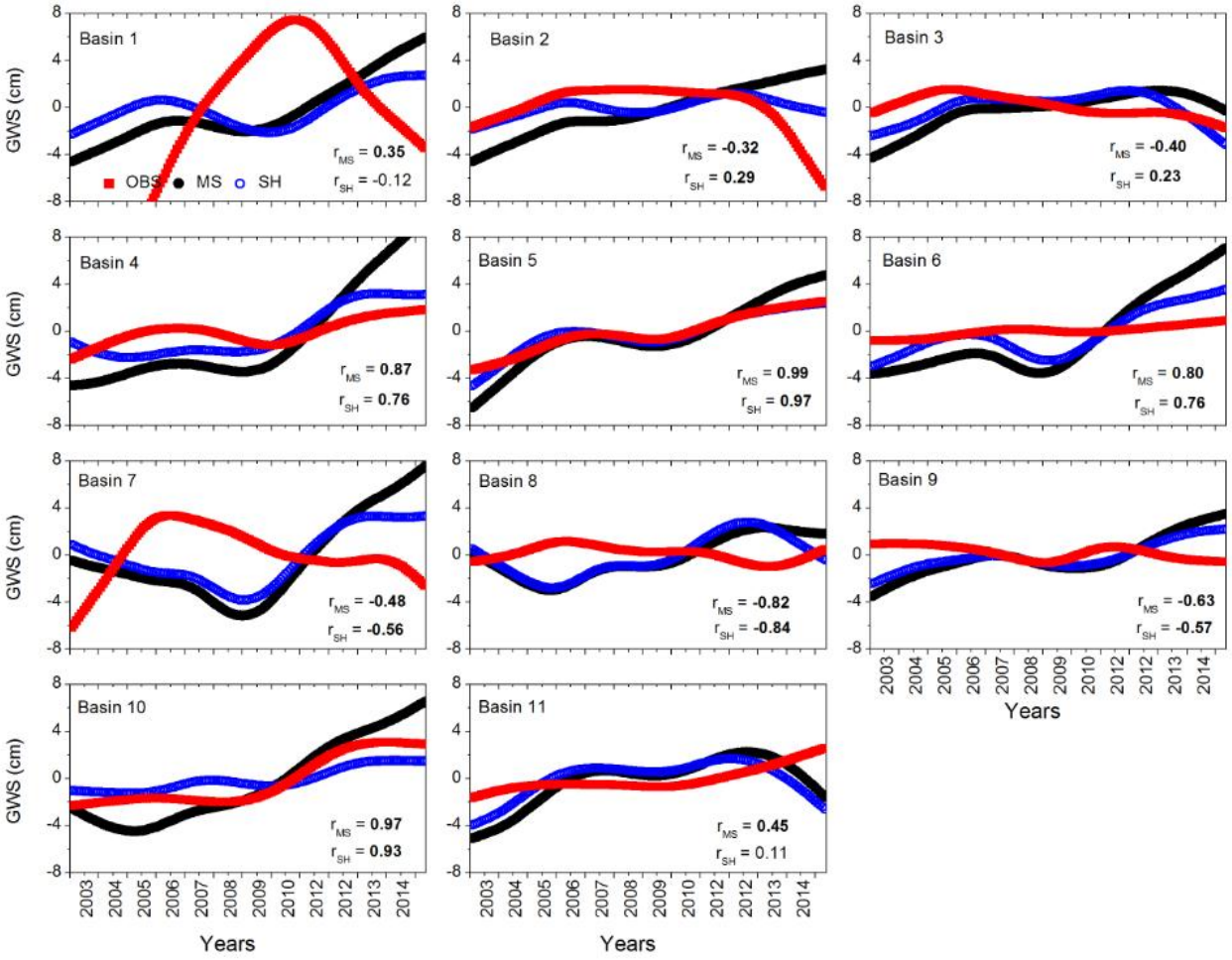

Figure 7: Basin-wide time-series of HP filter data for in situ GWSA (OBS, red squares), GWSA obtained using GRACE mascon product (MS, black filled circles) and GRACE SH products (SH, blue open circles), respectively. Pearson's correlation coefficient values are provided in in-set and statistically significant (*p value* < 0.01) values are shown in bold font

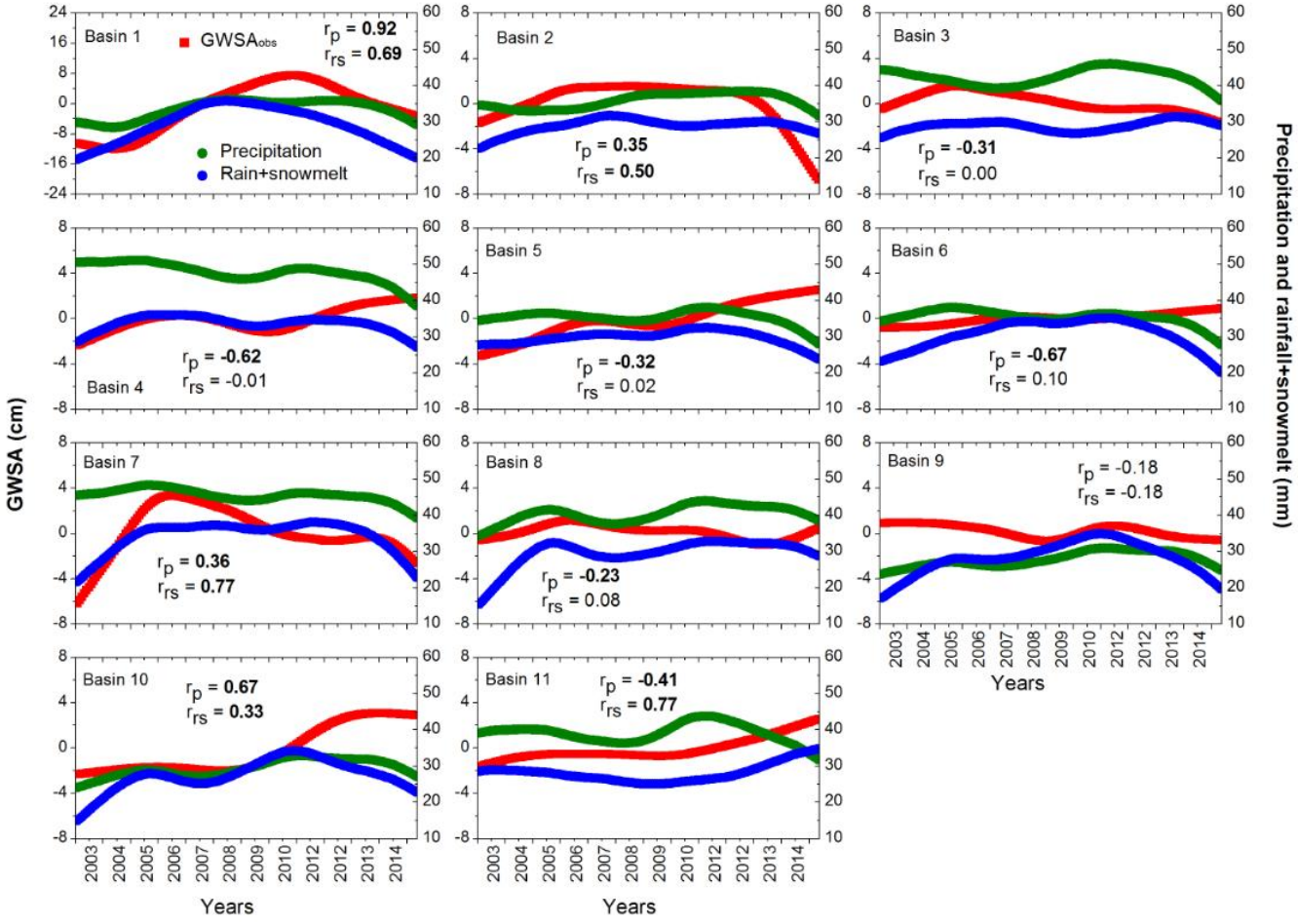

Figure 8: Basin-wide time-series of HP filter data for in situ GWSA (OBS, red squares), precipitation data (green circles) and rainfall+snowmelt data (blue circles). Pearson's correlation coefficient (r) values are provided in in-set and statistically significant (*p value* < 0.01) values are shown in bold font. r_p and r_{rs} indicate correlation between GWSA, and precipitation and rainfall+snowmelt, respectively

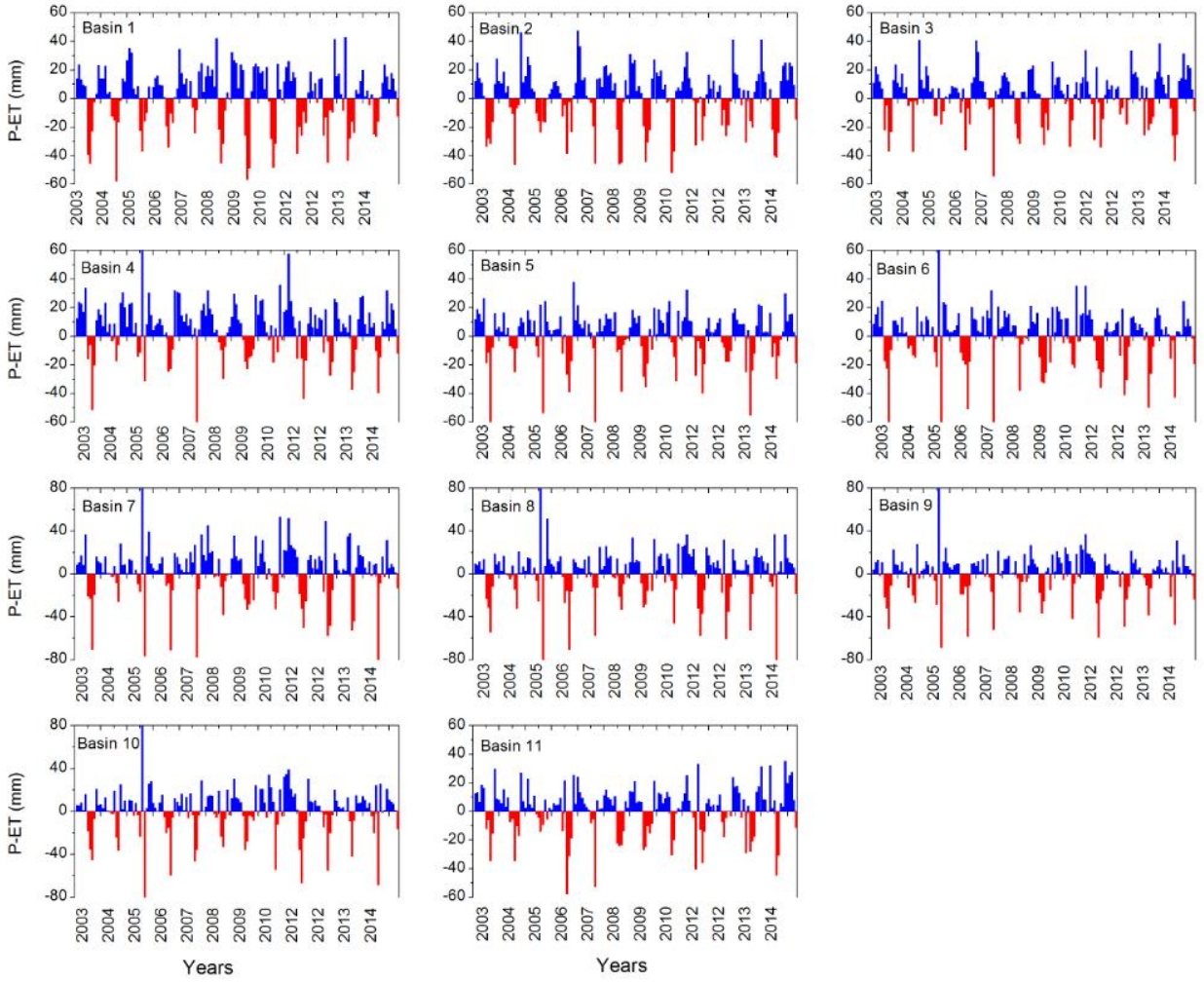

Figure 9: Basin-wide time-series of P – ET values. Positive values are shown in blue colour and negative values are shown in red colour

Table 1: Details of the river basins used (within Alberta only), number of wells used, precipitation, $GWSA_{obs}$ trends (statistically significant (*p value*< 0.01) trend estimates are shown in bold font) and P - ET trends in 2003-2015

Basin ID	Basin name	Ocean	Basin Area (m^2)	Number of wells	Precipitation (mm/year)	$GWSA_{obs}$ trends (cm/year)	P - ET trends (km^3 in 2003-2015)
1	Hay River Basin	Arctic Ocean	66196942347	3	401	**1.22**	-0.17
2	Peace River	Arctic	213025952509	15	429	-0.19	-0.41

	Basin	Ocean					
3	Athabasca River Basin	Arctic Ocean	144499671762	8	508	**-0.19**	-0.17
4	North Saskatchewan River	Hudson Bay	57046775461	21	573	**0.21**	-0.25
5	Battle River Basin	Hudson Bay	36561280700	28	424	**0.43**	-0.06
6	Red Deer River Basin	Hudson Bay	50024664775	21	425	**0.12**	-0.11
7	Bow River Basin	Hudson Bay	25639800168	15	546	-0.04	-0.08
8	Oldman River Basin	Hudson Bay	27023265616	10	486	-0.08	-0.03
9	South Saskatchewan River Basin	Hudson Bay	13504374212	6	334	**-0.10**	-0.01
10	Milk River Basin	Hudson Bay	11833516877	9	353	**0.52**	0.00
11	Beaver River Basin	Hudson Bay	16904014071	21	469	**0.24**	0.01